Published in final edited form as:
J Am Chem Soc. 2013 March 27; 135(12): 4735–4742. doi:10.1021/ja311641b.

Dynamics of Site Switching in DNA Polymerase

Rajan Lamichhane, **Svitlana Y. Berezhna**, **Edwin Van der Schans**, and **David P. Millar**
Department of Integrative Structural and Computational Biology, The Scripps Research Institute, 10550 N. Torrey Pines Rd., La Jolla, CA 92037

Abstract

DNA polymerases replicate DNA by catalyzing the template-directed polymerization of deoxynucleoside triphosphate (dNTP) substrates onto the 3′ end of a growing DNA primer strand. Many DNA polymerases also possess a separate 3′–5′ exonuclease activity that is used to remove misincorporated nucleotides from the nascent DNA (proofreading). The polymerase (pol) and exonuclease (exo) activities are spatially separated in different enzyme domains, indicating that a mechanism must exist to transfer the growing primer terminus from one site to the other. Here we report a single-molecule Forster resonance energy transfer (smFRET) system that directly monitors the movement of a DNA substrate between the pol and exo sites of DNA polymerase I Klenow fragment (KF). FRET trajectories recorded during the encounter between single polymerase and DNA molecules reveal that DNA can channel between the pol and exo sites in both directions while remaining closely associated with the enzyme (intramolecular transfer). In addition, it is evident from the trajectories that DNA can also dissociate from one site into bulk solution and subsequently rebind at the other (intermolecular transfer). Rate constants for each pathway have been determined by dwell-time analysis, revealing that intramolecular transfer is the faster of the two pathways. Unexpectedly, a mispaired primer terminus accesses the exo site more frequently when dNTP substrates are also present in solution, which is expected to enhance proofreading. Together, these results explain how the separate pol and exo activities of KF are physically coordinated to achieve efficient proofreading.

DNA polymerases replicate DNA rapidly and with extraordinary accuracy. The high fidelity is a result of selection of the correct dNTP substrate (complementary to the template base) during each cycle of template-directed polymerization, coupled with post-synthetic proofreading of misincorporated nucleotides by a separate 3′–5′ exonuclease activity[1]. Proofreading enhances the overall fidelity of DNA synthesis by a factor of 10–300, depending on the specific DNA polymerase and the nature of the primer terminal mispair[2,3]. The functional importance of proofreading is highlighted by observations that reduced 3′–5′ exonuclease activity of DNA polymerases is correlated with an increased mutation frequency *in vivo*[4–6].

Structural studies of several DNA polymerases, including members of the A, B and C polymerase families, indicate that the polymerase (pol) and 3′–5′ exonuclease (exo) activities are spatially separated in different enzyme domains[7–12], raising the question of how they work together to achieve accurate and efficient DNA replication (Fig. 1). Previous biochemical studies performed under conditions that enable observations of a single encounter between the polymerase and DNA substrate imply that the enzyme can switch from polymerization to 3′–5′ exonuclease activity without dissociation of the complex, suggesting that the primer 3′

Corresponding author: David P. Millar, Department of Integrative Structural and Computational Biology, The Scripps Research Institute, 10550 N. Torrey Pines Rd., La Jolla, CA 920137. Tel: (858) 784-9870. millar@scripps.edu.

terminus can channel between the respective active sites[13–17]. However, such channeling has not been directly observed within a single enzyme-DNA complex.

Here we describe a smFRET system that directly monitors movement of a DNA substrate between the spatially distinct pol and exo sites of KF. Our results reveal two distinct mechanisms for DNA site switching during proofreading. We have also quantified the microscopic rate constants for each transfer pathway and elucidated the influence of mismatch location within the DNA substrate on the switching kinetics. We further demonstrate that dNTPs specifically accelerate pol-to-exo switching of a mispaired DNA terminus, suggesting an expanded role for nucleotides in DNA polymerase function.

RESULTS

Detection of pol and exo site complexes by smFRET

The smFRET system utilizes a primer/template duplex labeled with an Alexa-Fluor 488 (A488) donor dye in the primer strand (Table 1) and a KF construct labeled with an Alexa-Fluor 594 (A594) acceptor at a mutated residue (K550C) in the thumb subdomain (Fig. 1). The KF construct also contains a C907S mutation to remove the single native cysteine and a D424A mutation that eliminates 3′–5′ exonuclease activity[18]. This construct will be referred to henceforth as wild type KF. The use of an exonuclease-deficient enzyme creates a system that is specifically designed to monitor the transfer of the DNA substrate between the pol and exo sites of the enzyme prior to the exonucleolytic excision step. Most experiments utilized a primer/template in which the 3′ terminal base of the primer strand (G) was mispaired with the corresponding base of the template (G), thereby mimicking the product of a misincorporation reaction (1 mm, Table 1). In addition, some experiments were performed using a fully matched primer/template (0 mm, Table 1), or a primer/template containing an internal mismatch (+1 mm, Table 1).

Primer/templates were immobilized on a quartz slide by biotin-avidin attachment and visualized at the single-molecule level by TIRF microscopy as they interacted with KF molecules present in solution. A typical pair of fluorescence intensity time traces, recorded with 100 ms integration time, shows perfectly anti-correlated jumps in the donor and acceptor channels (Fig. 2a, upper panel), indicating that the intensity jumps arise from changes in FRET efficiency rather than unrelated photophysical changes within either the donor or acceptor. The corresponding FRET efficiency trajectory reveals abrupt transitions as individual KF molecules repeatedly bind to and spontaneously dissociate from the immobilized DNA (Fig. 2a, lower panel). In addition, multiple transitions are observed between two distinct FRET states (~ 0.65 and ~ 0.8 FRET efficiencies) during the periods that KF is bound (Fig. 2a). These transitions are clearly resolved in trajectories recorded with faster time resolution (33 ms integration time, Fig. 2b).

A histogram of FRET efficiencies compiled from 230 trajectories reveals a broad asymmetric distribution (Fig. 2c, upper panel). The histogram can be fitted with two Gaussian functions, centered at 0.80 and 0.67 FRET efficiencies, confirming that two distinct FRET states are present. Based on the areas enclosed by each Gaussian peak, the lower FRET species accounts for 40% of the total population. The state at high FRET efficiency was previously assigned to DNA bound at the pol site of wt KF (labeled at residue 550, as here) [19]. To probe the origin of the lower FRET state, we introduced a L361A mutation into KF, which is known to disrupt DNA binding to the exo site[20]. The histogram for the L361A KF mutant reveals just a single peak centered at 0.79 FRET efficiency (Fig. 2c, lower panel). Hence, the lower FRET species observed with wt KF likely represents a subpopulation of complexes in which the DNA primer terminus is bound at the exo site.

To provide additional support for the proposed assignment of the lower FRET state, we performed similar smFRET measurements with a fully matched primer/template (0 mm, Table 1). A fully matched primer/template is expected to bind predominantly at the pol site of KF[21]. Consistent with this, the FRET histogram for wt KF interacting with the 0 mm primer/template reveals a major peak centered at 0.82 efficiency, with a shoulder at 0.67 efficiency accounting for just 10% of the total population (Fig. S1, Supporting Information). Together with Fig. 2c, these results demonstrate that the fractional population of the lower FRET state is correlated with the number of terminal mismatches within the DNA primer/template, increasing from 10% for no mismatches to 40% for a single mismatch. This trend is fully consistent with previous ensemble fluorescence anisotropy decay studies with dansyl-labeled DNA, which reveal that 7–14% of fully matched primer/templates or 18–37% of primer/templates containing a single terminal mismatch are bound at the exo site of KF, depending on the specific mismatch or terminal base pair and the surrounding DNA sequence[21]. Taken together, the results for the L361A KF mutant and the two different primer/templates definitively establish the assignment of the lower FRET state to a subpopulation of DNA bound at the exo site.

Control experiments were performed to determine whether the apparent change in FRET efficiency between the pol and exo site complexes was influenced by changes in the intrinsic quantum yield of the donor or acceptor or by changes in the orientation factor for energy transfer. To address the first question, the A488 emission intensity of immobilized DNA primer/template (1 mm, Table 1) was recorded over time in the presence or absence of unlabeled wt KF. Representative time traces (Fig. S2) show the A488 emission intensity is constant over time until an abrupt single-step photobleaching event occurs, regardless of whether unlabeled KF is present or absent, and that the mean intensity is similar in both conditions. Notably, the absence of detectable intensity jumps prior to photobleaching indicates that the A488 intensity remains constant as unlabeled KF binds to the DNA or as the DNA switches between the pol and exo sites. Hence, the intrinsic quantum yield of the A488 donor must be similar at each site. Similar TIRF experiments were performed with unlabeled DNA primer/template (1 mm) in the presence of A594 labeled wt KF, with direct excitation of the A594 dye using a 532 nm laser. In this experiment, the A594 emission is only detected while KF is bound to the immobilized DNA within the TIRF field. An intensity histogram compiled from 120 individual time traces reveals a relatively narrow major peak, with a very small shoulder at higher intensity (Fig. S3a). The shoulder corresponds to twice the intensity of the major peak, suggesting that a small fraction of complexes (< 5 %) contain two KF molecules bound to DNA. Importantly, the absence of any detectable splitting of the major peak implies that the A594 emission intensity is similar, regardless of whether the DNA is bound at the pol or exo sites (the 1 mm DNA partitions between both sites, as noted above). Consistent with this, the steady-state emission intensities of mixtures of A594-KF (25 nM) with unlabeled primer/templates (0 mm or 1 mm, 500 nM each) are essentially identical (within 1%). Since these primer/templates partition differently between the pol and exo sites, as shown above, the intrinsic acceptor intensity must be similar at each site. Hence, the gamma factor used to calculate the apparent FRET efficiencies (Materials and Methods) must be similar for the pol and exo site populations.

Lastly, to assess any changes in the orientation factor for energy transfer, we determined the bulk steady-state fluorescence anisotropy of the A488 and A594 probes under various conditions. The anisotropy of A488 was measured in a mixture of labeled primer/template (25 nM, either 1 mm or 0 mm, Table 1) with a saturating concentration of unlabeled wt KF (500 nM). The resulting values are 0.23 ± 0.01 and 0.25 ± 0.01, respectively. Since the 1 mm and 0 mm primer/templates partition differently among the pol and exo sites, the similarity of these values implies that the donor anisotropy does not change significantly between the pol and exo sites. Likewise, we measured the A594 anisotropy in mixtures of A594-labeled wt KF (25 nM)

with saturating concentrations of unlabeled primer/templates (500 nM, either 0 mm or 1 mm). The resulting value is 0.34 ± 0.01 in both cases, implying that the acceptor anisotropy is insensitive to whether the DNA is bound at the pol site or exo site. Since the anisotropy of both donor and acceptor appear to be independent of the site of DNA binding (pol site or exo site), the orientation factor for energy transfer is unlikely to change as DNA switches between the two sites.

In view of these control experiments, the change in FRET efficiency between the pol and exo site complexes must be due to a change in donor-acceptor distance, rather than a change in donor quantum yield, the gamma factor or the orientation factor. The apparent donor-acceptor distances for the pol and exo complexes are 42.9 Å and 48.0 Å, respectively, assuming a Förster radius of 54 Å for the A488/A594 pair (based on a value of 2/3 for the orientation factor) [22]. Both distances are apparent values, since they are calculated assuming a gamma factor of 1 and an orientation factor of 2/3. However, while the true gamma factor may differ from 1, or the orientation factor may differ from 2/3, these factors must have the same values for the pol and exo bound species, as noted above. Accordingly, it is meaningful to compare the two apparent distances. Both distances contain an unknown contribution from the linkers attaching the donor and acceptor dyes to the DNA and protein, respectively. If the linker contributions are assumed to be constant, the results suggest that the distance between the labeled primer base and the thumb subdomain of Pol I KF increases by ~ 5 Å as the primer/template switches from the pol site to the exo site. To obtain a refined estimate, we took into account the minimum and maximum values of the orientation factor that are compatible with the measured anisotropy of the donor and acceptor, and recalculated the donor-acceptor distances accordingly[23]. From this analysis, the estimated change in the inter-probe distance between the pol and exo site complexes is between 4.2 Å and 6.6 Å. This change in distance could be due to movement of the upstream DNA duplex, movement of the thumb subdomain or a combination of both.

Two modes of site switching

The smFRET trajectories reveal information about the kinetic pathways connecting the pol and exo site complexes and the associated rate constants. To illustrate this, we analyzed the set of 230 trajectories obtained for wt KF interacting with the 1 mm primer/template by Hidden Markov modeling, using the program HaMMy[24], and then constructed a two-dimensional plot of transition probability density (TPD) in which the starting FRET efficiency is plotted versus the final FRET efficiency for every individual transition in the data set, using the program TDP[24]. The resulting plot shows two clearly resolved regions on the y-axis (Fig. 2d), corresponding to transitions from unbound DNA (zero-FRET) to either the exo site complex (~ 0.65 FRET) or pol site complex (~ 0.8 FRET), indicating that DNA can bind directly to either site. The on-rates for binding to each site (0.27 ± 0.01 s^{-1} for the pol site and 0.25 ± 0.01 s^{-1} for the exo site) were obtained from dwell-time analysis (Figs. S4a and S4b). The similarity of these on-rates implies that the pol and exo sites are equally accessible for DNA binding. The on-rates correspond to bimolecular association rate constants of 5.4 ± 0.2 × 10^7 M^{-1} s^{-1} for the pol site and 5.0 ± 0.2 × 10^7 M^{-1} s^{-1} for the exo site at the KF concentration used (5 nM), values that are in the range expected for a diffusion-controlled binding process. The corresponding dissociation transitions from both pol and exo sites are also clearly resolved in the TPD plot along the x-axis (Fig. 2d). DNA dissociates more slowly from the pol site (rate constant 0.76 ± 0.03 s^{-1}, Fig. S4c) than from the exo site (rate constant 2.1 ± 0.1 s^{-1}, Fig. S4d), suggesting that more DNA-protein contacts are formed at the pol site. This conclusion is consistent with cocrystal structures of polymerase-DNA complexes, which reveal that the pol site interacts with both strands of the primer/template[25], while the exo site interacts mostly with the primer strand[7]. On the basis of these association and dissociation rate constants, we calculated the corresponding equilibrium dissociation constants: K_d = 14 ± 1 nM for the pol site complex and K_d = 42 ± 2 nM for the exo site complex. Using these values for the individual

binding sites, an overall dissociation constant was calculated as follows: $K_d = (1/14 + 1/42)^{-1} = 10.5 \pm 0.7$ nM. This calculated value is in good agreement with the equilibrium dissociation constant of 10 ± 2 nM obtained from a bulk fluorescence anisotropy titration of 1 mm primer/template with unlabeled wt KF (Fig. S5). Hence, the single-molecule kinetic data are fully consistent with the bulk equilibrium behavior.

The most prominent features of the TPD plot are the regions of high probability density for transitions connecting the two bound FRET states (Fig. 2d). These cross peaks suggest that the DNA substrate can transfer directly from the pol site to exo site (and vice versa). Dwell-time analysis indicates that DNA switches from the pol site to the exo site with a rate constant of $1.50 \pm 0.04\ s^{-1}$ (Fig. 3a) and returns to the pol site with a rate constant of $3.5 \pm 0.1\ s^{-1}$ (Fig. S4e). All the kinetic rate constants for dissociation and site switching determined in this study are summarized in Table 2.

Together, these results indicate that DNA can transfer between the pol and exo sites by two different pathways. First, DNA can dissociate from the pol site into bulk solution and subsequently rebind to the exo site (or vice versa). Examples of these intermolecular transfer events can be seen in the FRET trajectory in Fig. 2a. Second, we observe many events in which the two bound populations appear to directly exchange without any intervening period of zero FRET efficiency, indicating no dissociation of the complex. These events are clearly resolved in the representative FRET trajectory shown in Fig. 2b and are the most frequent transitions observed in the TPD plot (Fig. 2d). It is formally possible, however, that KF dissociates from the DNA and rebinds (using the other binding site) within the integration time of the CCD camera recordings (33 ms for the fastest recordings), which would create the impression of a direct transition between the two sites. If so, rebinding of KF must occur within 33 ms, setting a lower limit for the binding rate of $30\ s^{-1}$. This value corresponds to a bimolecular association rate constant $> 6 \times 10^9\ M^{-1}s^{-1}$, which significantly exceeds the rate constant expected for diffusion-controlled binding of KF from bulk solution. Hence, it is unlikely that the pol to exo switching transitions represent unresolved dissociation and rebinding events. Another possibility is that the polymerase molecule bound at the primer 3′ terminus via the pol site dissociates into solution and is quickly replaced by a second enzyme molecule that happens to be associated with the same DNA molecule. This second molecule may engage the primer terminus via the exo site. However, the probability of two KF molecules occupying the same DNA molecule is 5% or less (Fig. S3a), which is too small to account for the highly frequent transitions between the two bound FRET states. Moreover, the rate of pol to exo switching would be the same as the rate of dissociation from the pol site ($0.76 \pm 0.03\ s^{-1}$) according to this scenario, whereas the actual switching rate is significantly faster ($1.50 \pm 0.04\ s^{-1}$). We conclude that these transitions arise from a single KF molecule that remains closely associated with the same DNA molecule as the primer terminus relocates from the pol site to the exo site (and vice versa). This pathway is therefore referred to as intramolecular transfer.

An internal mismatch accelerates pol-to-exo switching of DNA

We also examined a primer/template containing a single T•T mismatch adjacent to a correct G•C terminus, with the remaining sequence being identical to the original primer/template (+1 mm, Table 1). Dwell-time analysis of the smFRET trajectories indicates that the rate of intramolecular transfer of DNA from the pol to exo site (rate constant $3.9 \pm 0.1\ s^{-1}$, Fig. S6a, Table 2) is faster than observed for the DNA containing the terminal G•G mismatch ($1.50 \pm 0.04\ s^{-1}$). Previous biochemical studies suggest that a duplex DNA substrate must partially melt and unwind for the primer 3′ terminus to bind at the exo site of KF[26]. The internal mismatch may accelerate transfer of DNA to the exo site by decreasing the activation energy for local melting and strand separation. The DNA returns more slowly to the pol site (rate constant of $2.40 \pm 0.04\ s^{-1}$, Fig. S6b, Table 2) compared to the primer/template with a terminal

mismatch ($3.5 \pm 0.1\ s^{-1}$), which could reflect slow annealing of the strands when reforming the internal T•T mismatch.

Nucleotides accelerate pol-to-exo switching of DNA

During DNA replication, the polymerase is exposed to a pool of the four possible dNTP substrates. In a previous smFRET study, using a different acceptor-labeled KF construct, we showed that the presence of a correct dNTP substrate (complementary to the template base) caused a DNA primer/template to bind exclusively at the pol site of KF[19]. In that case, the primer terminus was properly base paired. Such a shift in favor of the pol site would be deleterious for proofreading if it also occurred for a primer/template with a mispaired primer terminus. To investigate this possibility, we repeated the smFRET measurements using wt KF and 1 mm primer/template in the presence of 1 mM dTTP, which is complementary to the dA template base (Table 1). The 2′, 3′ dideoxy modification of the primer terminus prevented covalent incorporation of dTTP. Unexpectedly, intramolecular transfer of DNA from the pol site to the exo site is significantly faster (rate constant $3.8 \pm 0.1\ s^{-1}$) in the presence of dTTP (Fig. 3b, Table 2). The DNA also dissociates more rapidly from the pol site (rate constant of $1.48 \pm 0.03\ s^{-1}$, Fig. S7a, Table 2) under these conditions, thereby accelerating the intermolecular transfer pathway as well. In contrast, the rate constants for dissociation of DNA from the exo site ($2.5 \pm 0.1\ s^{-1}$, Fig. S7b) or transfer from the exo to pol site ($4.2 \pm 0.1\ s^{-1}$, Fig. S7c) are largely unaffected by the presence of dTTP (Table 2). Hence, dTTP exerts an effect at the pol site only, where dNTP substrates are expected to bind, apparently loosening contacts between the polymerase and the DNA substrate, resulting in faster dissociation or transfer to the exo site. Importantly, the presence of dTTP has no effect on the intrinsic donor or acceptor emission intensities (Figs. S2c and S3b, respectively). Moreover, dTTP has no effect on the donor anisotropy for the 1 mm primer/template bound to unlabeled KF (0.22 ± 0.01 in the absence of dTTP, 0.21 ± 0.01 in the presence of 1 mM dTTP) or the acceptor anisotropy of wt KF bound to unlabeled 1 mm primer/template (0.34 ± 0.01 in the presence or absence of 1 mM dTTP). Hence, the presence of dTTP does not appear to alter the photophysical or rotational properties of either the donor or acceptor probes.

Interestingly, these effects are not specific to dTTP, since similar results were obtained in the presence of dATP, which is mismatched with the dA template base. In fact, dATP appears to be more destabilizing than dTTP, causing faster switching from the pol to exo site (rate constant $4.9 \pm 0.1\ s^{-1}$, Fig. 3c, Table 2) and more rapid dissociation from the pol site (rate constant $2.40 \pm 0.03\ s^{-1}$, Fig. S8, Table 2). This additional destabilization at the pol site may reflect the nascent mispairing between the incoming dATP and the dA template base. Other rate constants are listed in Table 2. Overall, these results indicate that, rather than interfering with proofreading, the presence of dNTP substrates, either correct or incorrect, should actually enhance proofreading by accelerating transfer of a mispaired primer terminus from the pol site to the exo site.

The effects of dTTP just described are specific to a mispaired primer terminus. Representative smFRET trajectories for mispaired and fully paired primer/templates interacting with wt KF, both in the presence of dTTP, are shown in Figs. 3d and 3e, respectively. It is evident that fast pol-exo switching transitions are only observed when the primer terminus is mispaired. In contrast, the fully paired primer/template remains in the pol site (~ 0.8 FRET) for extended periods of time (exceeding 5 sec) in the presence of dTTP and does not switch to the exo site. Importantly, the only difference between the two experiments is the identity of the terminal base pair: G•G in Fig. 3d *versus* G•C in Fig. 3e.

DISCUSSION

This study has provided new insights into the mechanisms by which the separate polymerase and 3′–5′ exonuclease activities of KF are physically coordinated (Fig. 4). A KF molecule bound to DNA via the pol site can dissociate into bulk solution and then rebind utilizing the exo site (intermolecular transfer). Likewise, a KF molecule initially engaged with DNA via the exo site can dissociate into solution and rebind via the pol site. In addition, we have observed a second pathway in which the DNA substrate switches between the pol and exo sites while remaining associated with the same KF molecule. The existence of this intramolecular transfer pathway explains previous biochemical experiments that show that DNA polymerases, including KF, can execute both polymerization and proofreading reactions during a single encounter with a DNA substrate[13–17]. Intramolecular transfer of DNA from the pol site to exo site (rate constant $1.50 \pm 0.04\ s^{-1}$) is faster than the corresponding intermolecular pathway, which is governed by the relatively slow rate of dissociation of DNA from the pol site (rate constant $0.76 \pm 0.03\ s^{-1}$). Similarly, intramolecular switching of DNA from the exo site to the pol site (rate constant $3.5 \pm 0.1\ s^{-1}$) is faster than dissociation from the exo site into bulk solution (rate constant $2.1 \pm 0.1\ s^{-1}$). Notably, transfer of DNA from the pol site to the exo site by either pathway is much faster than the rate of extension from a mispaired primer terminus (0.027 s^{-1} for KF[27]), explaining why exonucleolytic proofreading is effective in removing misincorporated nucleotides.

In view of the wide spatial separation of the pol and exo sites in KF (Fig.1), a substantial rearrangement of the enzyme-DNA complex must occur during the transition from polymerization to proofreading activity. Previous biochemical studies of KF suggest that partial unwinding and strand separation of the primer/template is required for 3′–5′ exonuclease activity[26]. In addition, fluorescence-based CD spectroscopic studies of KF interacting with primer/templates containing fluorescent base analogs indicate that the primer terminus is bound to the exo site in an extended single-stranded conformation[28]. This requirement for duplex melting is also consistent with our results showing faster pol to exo transfer for DNA containing an internal mismatch compared with a terminal mismatch. The internal mismatch is expected to be more disruptive and to promote fraying of the primer terminus. In addition to duplex melting, biochemical studies employing a DNA primer/template containing a steric blocking group (biotin) indicate that KF adopts different positions on DNA during polymerization or 3′–5′ exonuclease activity[26]. This is consistent with our smFRET results showing that the distance between the upstream duplex and the thumb subdomain increases by ~ 5 Å during the transition from the pol site to the exo site. We performed a series of control experiments to confirm that the difference in FRET efficiency between the pol and exo site complexes is actually due to this distance change. However, the cocrystal structures shown in Fig. 1 suggest that the donor-acceptor distance would increase by only 0.6 Å during pol to exo switching (based on distances between the C5 position of the labeled primer base and the C_β atom of the labeled amino acid in the thumb subdomain), a change that is too small to give rise to any detectable difference in FRET efficiency. This discrepancy is likely a consequence of the unnatural 3′ single-stranded primer overhang within the DNA substrate used to obtain the exo bound complex shown in Fig 1 (right). In reality, the DNA substrate encountered during proofreading contains a single-stranded overhang on the template rather than primer stand.

On the basis of the smFRET observations presented here, together with the previous biochemical[26] and spectroscopic studies[28] indicating a requirement for localized duplex melting, we propose two mechanisms for intramolecular transfer of DNA from the pol site to exo site. First, the DNA duplex could spontaneously fray and transiently detach from the pol site, allowing the polymerase to diffuse stochastically on the DNA until the primer 3′ terminus engages the exo site. Alternatively, the enzyme may actively promote DNA strand separation

and guide the primer terminus to the exo site through a directed diffusion process. Our present results do not distinguish between these two scenarios. Future studies using the smFRET method and site-directed mutants of KF should be able to discriminate the two models and identify amino acid residues that promote strand separation and/or facilitate movement of the DNA substrate.

The results obtained in this study also provide novel insights into how KF recognizes and utilizes nucleotides. The presence of a correct dTTP substrate stabilizes DNA at the pol site and suppresses pol-exo switching when the primer terminus is correctly base paired (Fig. 3e). Preferential binding of matched DNA at the pol site under these conditions was also observed in our previous smFRET study using a different labeling scheme, although the dynamics of pol-exo site switching were not addressed in that study[19]. In contrast, the same dTTP substrate accelerates dissociation of DNA from the pol site and induces faster transfer of the primer terminus from the pol site to the exo site when the primer terminus is mispaired (Figs. 3b and 3d, Table 2), even though dTTP is complementary to the template base. Hence, dTTP has completely different effects, depending on the nature of the terminal base pair (correctly paired or mispaired). Interestingly, we observed that dATP also induces faster switching of the mispaired primer terminus from the pol site to the exo site, indicating that the ability of nucleotides to accelerate switching is a general phenomenon. In fact, dATP is more destabilizing than dTTP, inducing faster dissociation from the pol site (Fig. S8, Table 2) and more rapid transfer to the exo site (Fig. 3c, Table 2) than dTTP. This additional destabilization may arise from nascent mispairing between the incoming dATP and the dA template base.

Together, these results suggest a dual role for dNTPs during DNA polymerase activity. During extension of a properly paired primer terminus, dNTPs are utilized as substrates for 5′–3′ polymerization. Correct dNTPs induce the catalytically active closed conformation[19,29–31] and stabilize the polymerase on the DNA substrate[19]. In contrast, during proofreading of a mispaired primer terminus, any dNTP can act as a cofactor to stimulate transfer of the primer terminus from the pol site to the exo site. While the former role is well known, the ability of dNTPs to promote pol-to-exo switching has not been reported before to our knowledge. This phenomenon is the opposite of the previously reported “next-nucleotide effect”, whereby proofreading efficiency is reduced in the presence of the next required dNTP substrate[32]. The next-nucleotide effect arises from kinetic competition between 3′–5′ exonucleolytic hydrolysis and extension of a mispaired primer terminus, and is specific to a correct dNTP substrate. In contrast, we have identified a new effect of nucleotides that operates at the level of pol-to-exo switching, does not require nucleotide incorporation (blocked in our experiments by a 2′, 3′ dideoxy modification of the primer terminus) and occurs with both correct and incorrect dNTPs. Moreover, our results suggest that the functional role of a particular dNTP is dependent on the nature of the previously synthesized base pair (whether correctly paired or mispaired). These observations highlight the ability of KF to detect proper base pairing at the primer terminus and to respond to dNTPs according to the appropriate functional context.

CONCLUSIONS

Proofreading by an intrinsic 3′–5′ exonuclease activity is used by many DNA polymerases to enhance the fidelity of DNA synthesis. Structural studies of a variety of polymerases have revealed that the pol and exo sites are spatially separated, just as they are in KF[7,33], although the spatial relationship of the sites is quite different in polymerases from the B and C families[10–12], suggesting that the mechanisms for site switching of DNA must also differ. Nevertheless, the two sites are separated by more than 20 Å in all cases. It is not understood for any polymerase family how the primer terminus is able to traverse the large distance between the two active sites during proofreading. Models have been proposed on the basis of static crystal structures of polymerases from the A and B families[7,9,10,34], but little is known

about the dynamic movement and melting of DNA during site switching. In this study, we have reported the first direct observation of intramolecular site switching of DNA in any DNA polymerase and quantified the rate constants for transfer in both directions. The smFRET system provides a new tool to study the dynamics of this ubiquitous mechanistic process in real-time. Moreover, given the flexibility in placement of the donor and acceptor probes, it will be straightforward to adapt the system to polymerases from other polymerase families.

MATERIALS AND METHODS

Expression of KF derivatives

KF mutants carrying a K550C cysteine substitution or K550C/L361A substitutions were generated from the D424A/C907S KF genotype construct generously provided by Dr. Catherine Joyce (Yale University) using a QuickChange kit (Stratagene). The C907S and D424A mutations remove the single native cysteine and suppress $3'$–$5'$ exonuclease activity, respectively. Expression and purification of the KF mutants was carried out as described previously[35].

Protein labeling

KF constructs were labeled with Alexa-Fluor 594 maleimide (Invitrogen) and purifed, as described[19]. The purity and specificity of labeled KF constructs was characterized by SDS-PAGE and ESI–TOF mass-spectrometry (Agilent). The degree of labeling was typically 100% after FPLC purification. Protein concentrations were calculated based on the optical absorption measured at 280 nm using extinction coefficient $\varepsilon_{280} = 5.88 \times 10^4\ M^{-1}\ cm^{-1}$. The protein was stored at −80 °C in a buffer containing 10 mM Tris-HCl, pH 7.5, 1 mM EDTA, 1 mM DTT and 50 % (vol/vol) glycerol.

Oligonucleotides

All oligonucleotides were obtained from Eurofins MWG Operon or Integrated DNA Technologies, and were purified by denaturing electorphoresis in 20% (weight/vol) polyacrylamide gels. A dideoxy terminated primer strand was prepared, labeled with Alexa-Fluor 488 and purified by HPLC, as described[19].

smFRET measurements

smFRET data collection was performed using a custom built prism-based TIRF microscope based on an inverted Axiovert 200 microscope (Zeiss), as described[19]. Quartz slides were cleaned, passivated with polyethylene glycol and coated with streptavidin, as described[36]. Primer/template duplexes in imaging buffer (50 mM tris pH 7.5, 10 mM $MgCl_2$, 0.5 mg/ml BSA, 1 mM DTT and 2 mM trolox) were introduced into the sample chamber and allowed to bind to the streptavidin-coated surface. Binary complexes were formed by subsequently introducing 5 nM KF into the sample chamber. Nucleotides (1 mM dTTP or dATP) were subsequently added in some of the experiments. CCD camera imaging movies were acquired with 100 ms or 33 ms integration time. A custom written single-molecule data acquisition package (downloaded from https://physics.illinois.edu/cplc/software/) was used in combination with IDL (ITT VIS) to record data and generate matched pairs of donor and acceptor fluorescence intensity traces.

smFRET data analysis

Individual intensity trajectories from the donor and acceptor channels were corrected for their respective background signals and for leakage from the donor into the acceptor channel, as described[19]. The corrected intensity trajectories were used to calculate FRET efficiency trajectories, according to the formula $E = I_A/(\gamma I_D + I_A)$, where E is the FRET efficiency and

I_D and I_A are the donor and acceptor intensities, respectively, and γ is a correction factor that accounts for differences in quantum yield and detection efficiency between donor and acceptor. Since γ was set to unity, the reported FRET efficiencies are apparent rather than absolute values. Each trajectory was processed using custom code written in MATLAB, as described previously[37,38]. Only trajectories exhibiting anti-correlated fluctuations of the donor and acceptor emission and single-step photobleaching were selected for further analysis. The FRET traces were smoothed by 3-point sliding averaging and then binned to generate a FRET histogram for each analyzed time trace and a composite FRET histogram was then compiled from multiple trajectories, using IGOR Pro (Version 6, WaveMetrics). Individual peaks in the FRET histograms were fitted with Gaussian functions, using IGOR Pro software, varying the peak position and width for best fit. In cases where a single Gaussian was insufficient, the histogram was fitted with two Gaussian functions, varying the peak position, width and amplitude of each peak for best fit. In some cases, noted in the figure captions, one of the peak positions was constrained. The area under each peak determined the percentage of complexes in the corresponding state. FRET time traces (not smoothed) were fitted with a hidden Markov model, using the program HaMMy, and two-dimensional plots of transition probability density were constructed using the program TDP, as described[24]. Histograms of dwell-times spent in each FRET state before transition to a different FRET state were compiled from the idealized FRET trajectories obtained from the HaMMy analysis. Kinetic rate constants were obtained by fitting the dwell-time histograms with a single exponential decay function, using IGOR Pro software.

Supplementary Material

Refer to Web version on PubMed Central for supplementary material.

Acknowledgments

We thank Catherine Joyce (Yale University) for the gift of plasmids and host cells, and Goran Pljevaljcic for assistance with data analysis. This study was supported by the National Institute of General Medical Sciences (grant GM044060 to D. P. M.).

REFERENCES

1. Kunkel TA. J Biol Chem. 2004; 279:16895. [PubMed: 14988392]
2. Kuchta RD, Benkovic P, Benkovic SJ. Biochemistry. 1988; 27:6716. [PubMed: 3058205]
3. Donlin MJ, Patel SS, Johnson KA. Biochemistry. 1991; 30:538. [PubMed: 1988042]
4. Reha-Krantz LJ, Bessman MJ. J Mol Biol. 1977; 116:99. [PubMed: 592387]
5. DiFrancesco R, Bhatnagar SK, Brown A, Bessman MJ. J Biol Chem. 1984; 259:5567. [PubMed: 6325441]
6. Tabor S, Richardson CC. J Biol Chem. 1989; 264:6447. [PubMed: 2703498]
7. Beese LS, Derbyshire V, Steitz TA. Science. 1993; 260:352. [PubMed: 8469987]
8. Doublie S, Tabor S, Long AM, Richardson CC, Ellenberger T. Nature. 1998; 391:251. [PubMed: 9440688]
9. Shamoo Y, Steitz TA. Cell. 1999; 99:155. [PubMed: 10535734]
10. Franklin MC, Wang J, Steitz TA. Cell. 2001; 105:657. [PubMed: 11389835]
11. Swan MK, Johnson RE, Prakash L, Prakash S, Aggarwal AK. Nat Struct Mol Biol. 2009; 16:979. [PubMed: 19718023]
12. Evans RJ, Davies DR, Bullard JM, Christensen J, Green LS, Guiles JW, Pata JD, Ribble WK, Janjic N, Jarvis TC. Proc Natl Acad Sci U S A. 2008; 105:20695. [PubMed: 19106298]
13. de Vega M, Blanco L, Salas M. J Mol Biol. 1999; 292:39. [PubMed: 10493855]
14. Fidalgo da Silva E, Reha-Krantz LJ. Nucleic Acids Res. 2007; 35:5452. [PubMed: 17702757]
15. Joyce CM. J Biol Chem. 1989; 264:10858. [PubMed: 2659595]

16. Reddy MK, Weitzel SE, von Hippel PH. J Biol Chem. 1992; 267:14157. [PubMed: 1629215]
17. Strick R, Knopf CW. Biochim Biophys Acta. 1998; 1388:315. [PubMed: 9858758]
18. Derbyshire V, Grindley ND, Joyce CM. EMBO J. 1991; 10:17. [PubMed: 1989882]
19. Berezhna SY, Gill JP, Lamichhane R, Millar DP. J Am Chem Soc. 2012; 134:11261. [PubMed: 22650319]
20. Lam WC, Van der Schans EJ, Joyce CM, Millar DP. Biochemistry. 1998; 37:1513. [PubMed: 9484221]
21. Carver TE Jr, Hochstrasser RA, Millar DP. Proc Natl Acad Sci U S A. 1994; 91:10670. [PubMed: 7938011]
22. Mukhopadhyay S, Krishnan R, Lemke EA, Lindquist S, Deniz AA. Proc Natl Acad Sci U S A. 2007; 104:2649. [PubMed: 17299036]
23. Dale RE, Eisinger J, Blumberg WE. Biophys J. 1979; 26:161. [PubMed: 262414]
24. McKinney SA, Joo C, Ha T. Biophys J. 2006; 91:1941. [PubMed: 16766620]
25. Johnson SJ, Taylor JS, Beese LS. Proceedings of the National Academy of Sciences. 2003; 100:3895.
26. Cowart M, Gibson KJ, Allen DJ, Benkovic SJ. Biochemistry. 1989; 28:1975. [PubMed: 2541768]
27. Carroll SS, Cowart M, Benkovic SJ. Biochemistry. 1991; 30:804. [PubMed: 1899034]
28. Datta K, Johnson NP, LiCata VJ, von Hippel PH. J Biol Chem. 2009; 284:17180. [PubMed: 19411253]
29. Rothwell PJ, Mitaksov V, Waksman G. Molecular Cell. 2005; 19:345. [PubMed: 16061181]
30. Santoso Y, Joyce CM, Potapova O, Le Reste L, Hohlbein J, Torella JP, Grindley NDF, Kapanidis AN. Proceedings of the National Academy of Sciences. 2010; 107:715.
31. Stengel G, Gill JP, Sandin P, Wilhelmsson LM, Albinsson B, Norden B, Millar D. Biochemistry. 2007; 46:12289. [PubMed: 17915941]
32. Kunkel TA, Schaaper RM, Beckman RA, Loeb LA. J Biol Chem. 1981; 256:9883. [PubMed: 6456268]
33. Freemont PS, Friedman JM, Beese LS, Sanderson MR, Steitz TA. Proc Natl Acad Sci U S A. 1988; 85:8924. [PubMed: 3194400]
34. Eom SH, Wang J, Steitz TA. Nature. 1996; 382:278. [PubMed: 8717047]
35. Joyce CM, Derbyshire V. Methods Enzymol. 1995; 262:3. [PubMed: 8594356]
36. Lamichhane R, Solem A, Black W, Rueda D. Methods. 2010; 52:192. [PubMed: 20554047]
37. Zhuang X, Kim H, Pereira MJ, Babcock HP, Walter NG, Chu S. Science. 2002; 296:1473. [PubMed: 12029135]
38. Rueda D, Bokinsky G, Rhodes MM, Rust MJ, Zhuang X, Walter NG. Proc Natl Acad Sci U S A. 2004; 101:10066. [PubMed: 15218105]

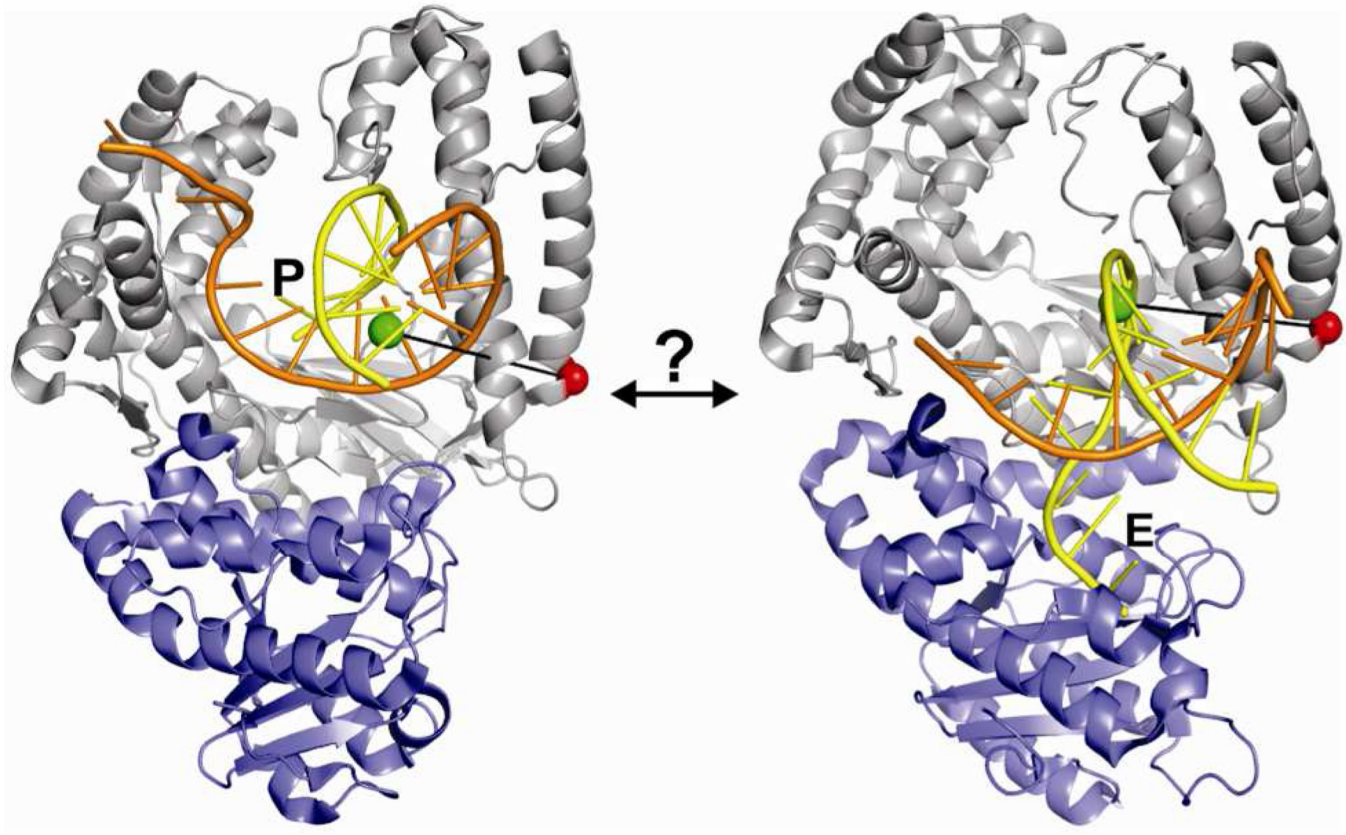

Figure 1.

Cocrystal structures of DNA polymerase bound to DNA. The structure on the left corresponds to the open binary complex of the KF homolog *Bst* Pol I and DNA[25] (PDB code 1L3S). The primer 3′ terminus is located in the pol site (P). The structure on the right is for a complex of KF with DNA bound at the exo site (E) [7] (PDB code 1KLN). In contrast to the structure shown on the left, the DNA contains a single-stranded extension on the primer strand rather than the template strand. In both structures, the primer strand is yellow, the template strand is orange, the polymerase domain is grey and the 3′–5′ exonuclease domain is aqua. The donor and acceptor probes used for smFRET measurements are shown as green and red spheres, respectively. The mechanism for transfer of DNA from the pol site to the exo site is not fully understood and is the subject of the present study.

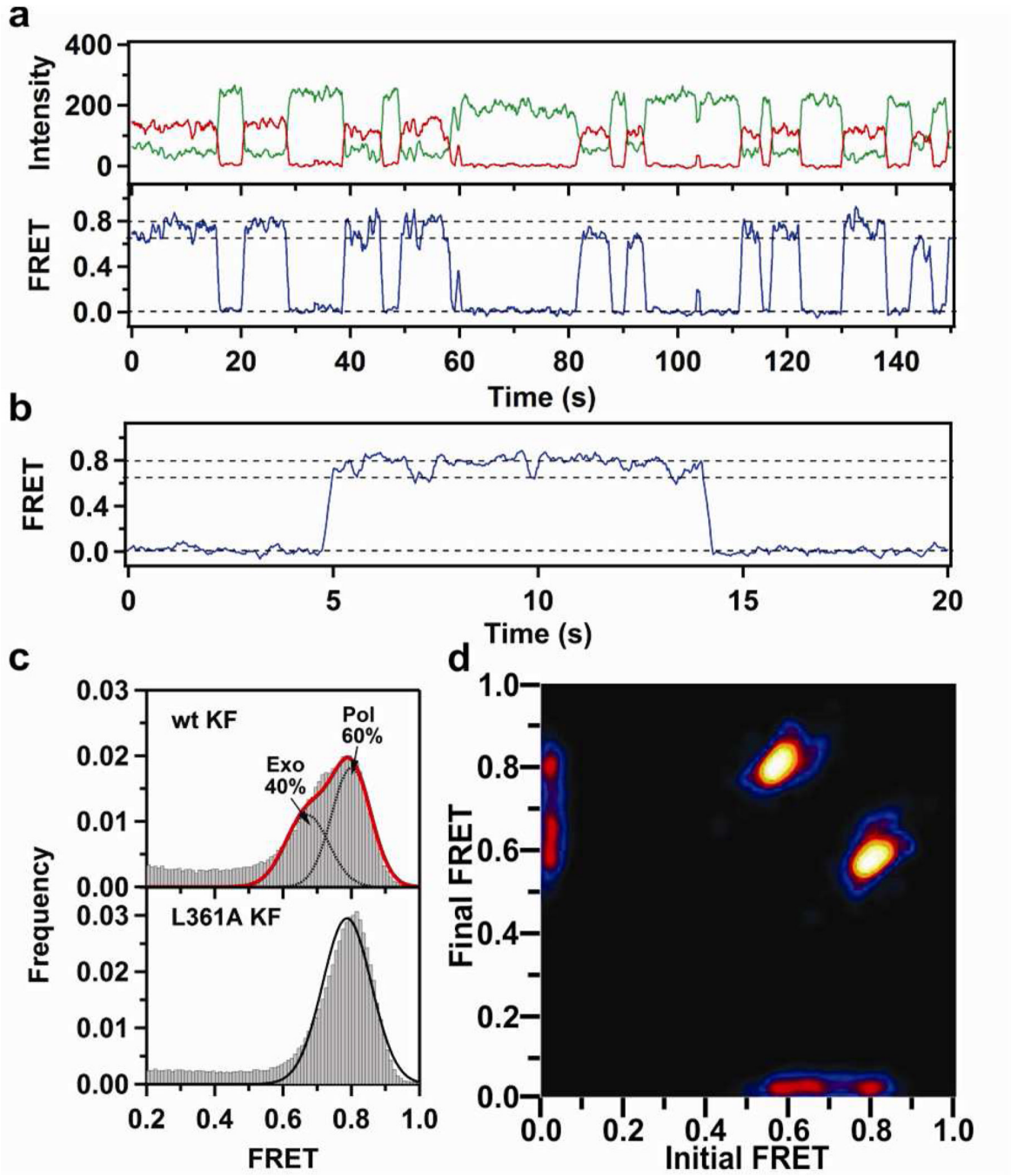

Figure 2.

Binding, dissociation and site switching of KF visualized by smFRET. The DNA contains a G•G mismatch at the primer 3′ terminus (1 mm, Table 1). (a) Time traces of the A488 donor (green) and A594 acceptor (red) emission intensity, recorded with 100 ms integration time. The corresponding FRET efficiency trajectory (blue) is shown in the lower panel. The dashed lines at 0, 0.65 and 0.80 FRET efficiencies correspond to unbound DNA, DNA bound at the exo site and DNA bound at the pol site, respectively. (b) FRET trajectory for the same sample recorded using 33 ms integration time, showing multiple pol-exo switching events. (c) Histogram of FRET efficiencies for wt KF (upper panel, compiled from 230 trajectories) and

L361A KF (lower panel, compiled from 261 trajectories), each interacting with the mispaired primer/template. In the upper panel, the dashed black lines are Gaussian fits to each peak and the red line is the composite fit to the overall histogram. The fitted centers and widths are 0.67 and 0.09, respectively, for the lower FRET peak, and 0.80 and 0.08, respectively, for the higher FRET peak. The fractional areas enclosed by each peak are indicated. In the lower panel, the black line is the best fit to a single Gaussian function, with fitted center and width of 0.79 and 0.10, respectively. (d) Transition probability density plot for wt KF interacting with the mispaired primer/template. The colored regions reveal connectivity between individual FRET states, with shading from blue to red to yellow indicating higher transition probability.

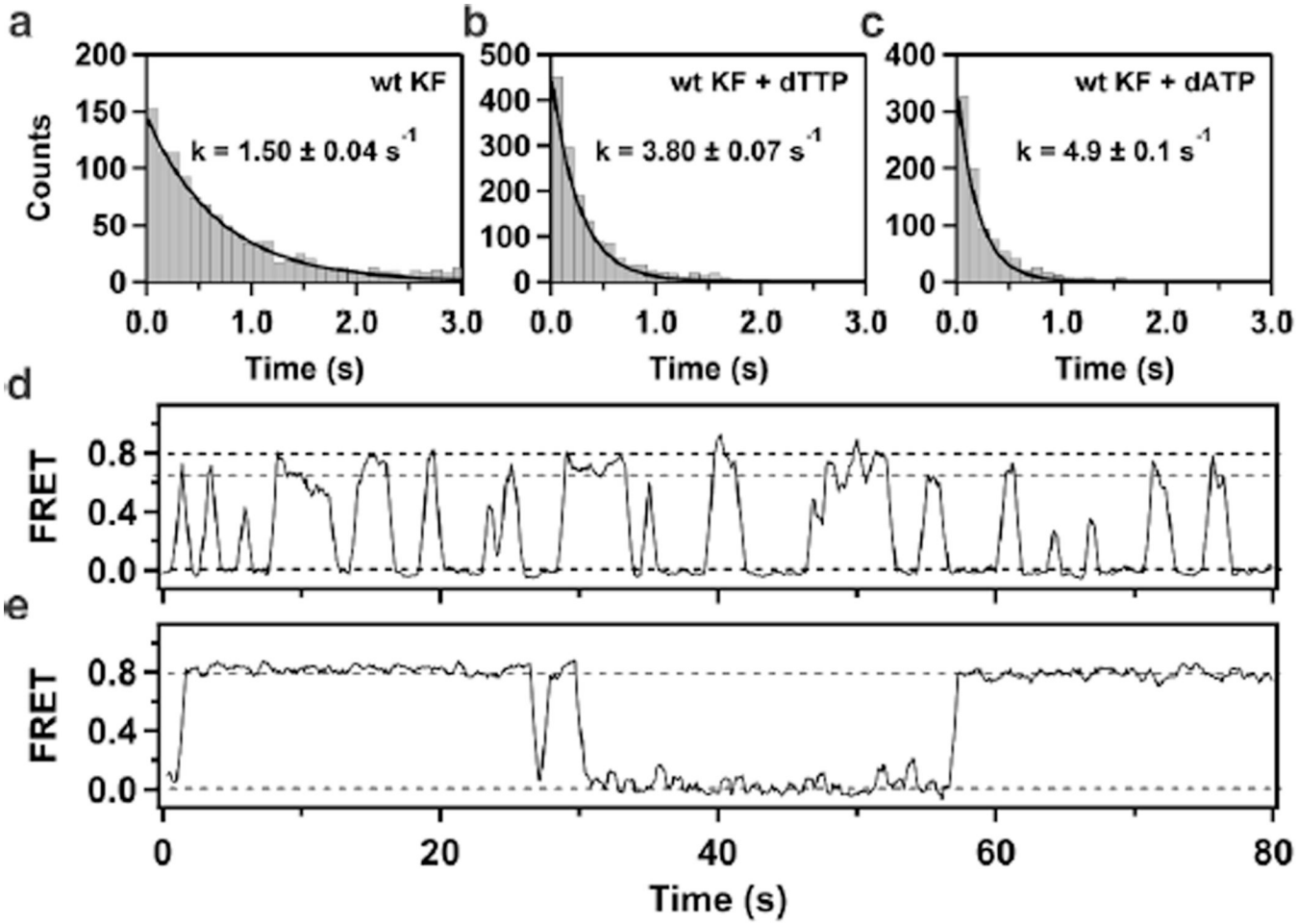

Figure 3.

Kinetics of intramolecular switching of DNA between the pol and exo sites of KF. (a) Histogram of dwell-times in the pol site before transition to the exo site for wt KF interacting with primer/template containing a terminal G•G mispair (1 mm, Table 1). The histogram is compiled from 1195 transitions. The solid line is the best fit to a single exponential function, with the indicated rate constant. (b) Corresponding dwell-time histogram (compiled from 1584 transitions) for wt KF interacting with the mispaired primer/template in the presence of 1 mM dTTP. The exponential fit line and corresponding rate constant are indicated. (c) Corresponding dwell-time histogram (compiled from 939 transitions) for wt KF interacting with the mispaired primer/template in the presence of 1 mM dATP. The exponential fit line and corresponding rate constant are indicated. (d) Representative smFRET trajectory for wt KF interacting with the mispaired primer/template in the presence of dTTP (1 mM). (e) Representative smFRET trajectory for wt KF interacting with fully base paired primer/template (0 mm, Table 1) in the presence of dTTP (1 mM). In (d) and (e), the dashed lines at 0, 0.65 and 0.80 FRET efficiencies correspond to unbound DNA, DNA bound at the exo site and DNA bound at the pol site, respectively.

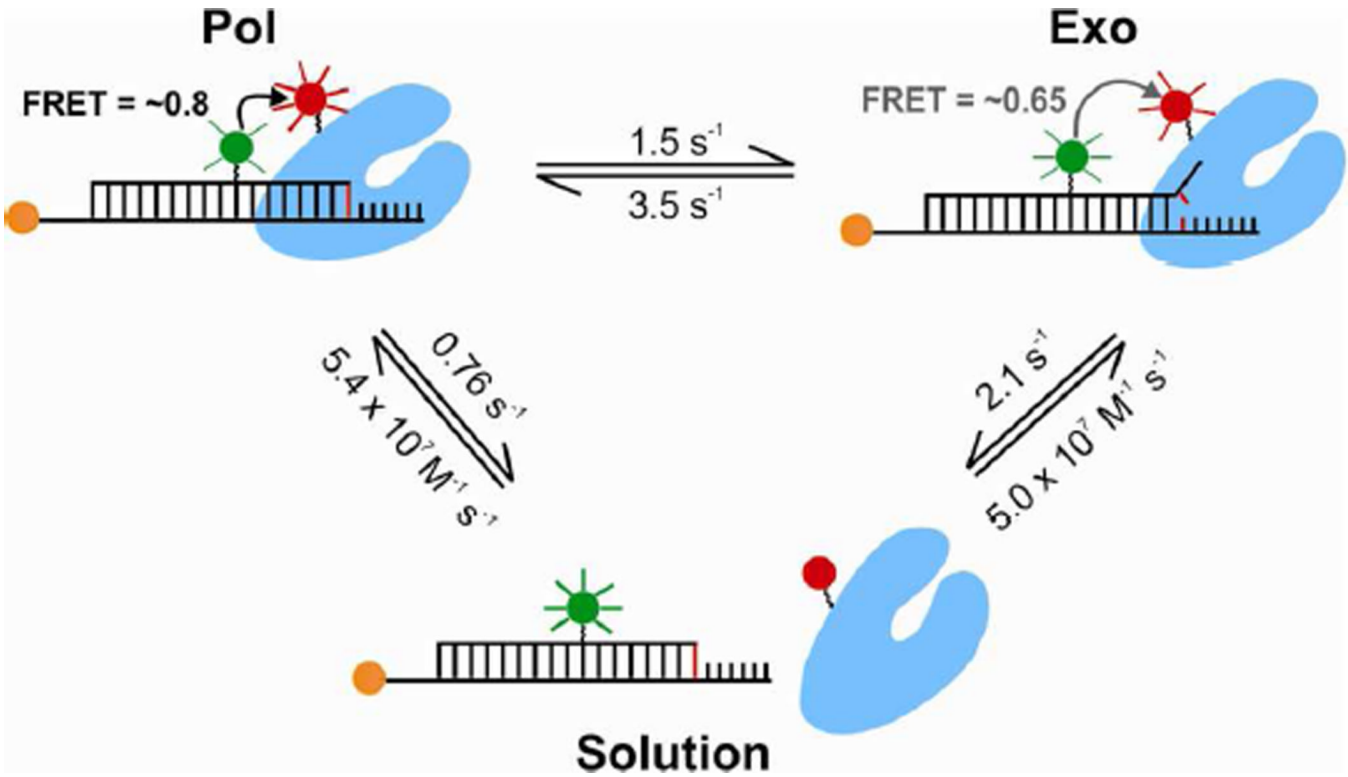

Figure 4.

Two pathways for switching of DNA between the pol and exo sites of KF as revealed by the present smFRET studies. The rate constants for each step in the two pathways are indicated. The orange circle at the end of the DNA primer/template represents the biotin group used for surface immobilization.

Primer/template	Sequence[a]
1 mm	5 TCGCAGCCGYCAATAT**G**$_H$ 3 3 B–T$_{30}$–AGCGTCGGCAGTTATA**G**ATATAGC 5
0 mm	5 TCGCAGCCGYCAATATC$_H$ 3 3 B–T$_{30}$–AGCGTCGGCAGTTATAGATATAGC 5
+1 mm	5 TCGCAGCCGYCAATA**T**G$_H$ 3 3 B–T$_{30}$–AGCGTCGGCAGTTAT**T**CATATAGC 5

[a]B denotes a biotin group used for surface attachment of the primer/templates, Y denotes an amino-dT residue labeled with Alexa-Fluor 488, and the subscript H denotes a 2′, 3′-dideoxy modification. Mismatched base pairs are denoted by bold type.

Table 2

Kinetic rate constants (s^{-1})

Primer/template	dNTP	Dissoc from pol site	Dissoc from exo site	pol-to-exo	exo-to-pol
1 mm	none	0.76 ± 0.03	2.1 ± 0.1	1.50 ± 0.04	3.5 ± 0.1
1 mm	dTTP	1.48 ± 0.03	2.5 ± 0.1	3.8 ± 0.1	4.2 ± 0.1
1 mm	dATP	2.40 ± 0.03	2.90 ± 0.01	4.9 ± 0.1	6.5 ± 0.1
+1 mm	none	2.4 ± 0.1	1.2 ± 0.1	3.9 ± 0.1	2.40 ± 0.04